

A SERS study of the galvanostatic sequence used for the electrochemical deposition of copper from baths employed in the fabrication of interconnects

Lucia D'Urzo · Benedetto Bozzini

Received: 29 December 2007 / Accepted: 14 March 2008 / Published online: 9 April 2008
© Springer Science+Business Media, LLC 2008

Abstract This paper reports the first study carried out by surface-enhanced Raman spectroscopy (SERS) during the galvanostatic electrodeposition (ECD) of copper from an acidic sulphate solution, in the presence of polyethylene glycol (PEG), bis-(3-sulfopropyl)-disulfide Na salt (SPS), benzyl-phenyl modified polyethyleneimine (BPPEI) and chloride ions. The analysis of SERS spectra recorded during electrodeposition allowed to get an insight into the complex interfacial behaviour of the organic blend, in terms of co-adsorption and reactivity. At open-circuit (OC), the additives co-adsorb on the copper cathode. Upon increasing the cathodic polarization, progressive SPS-scavenging action of PEG was observed. BPPEI is adsorbed in the entire process window and cathodic reaction products of PEG were identified. The joint action of the organic additives yields a continuous deposit with crystallites of submicron dimensions, as revealed by Scanning electron microscopy (SEM).

1 Introduction

Electroplated copper is becoming the electric contact material of choice in the semiconductor industry, because it offers lower line resistance and better electromigration performance compared to conventional Al and Al-alloy metallization [1]. As a consequence of the interaction of different organic additives and of special electrochemical polarisation schemes “superfilling” behaviour can be achieved, yielding void- and seam-free electrodeposits in high-aspect ratio features. The

organic additives in acid Cu plating baths are commonly categorised as [2–5]: (i) carriers or suppressors, (ii) brighteners or accelerators and (iii) levellers. Historically, Polyethylene glycol (PEG) of several molecular weights (MWs) [6–11] and Bis-(3-sulfopropyl)-disulfide Na salt (SPS) [12–30] were used in the Cu ECD as suppressor and accelerator, respectively. Nowadays, the selection of the levelling agent represents one of the crucial factors for an effective transition of Cu ECD towards the most advanced technology nodes. A novel polymeric leveller based on polyvinylpyrrolidone has been recently presented in [31]. In this paper we deal with copper electrodeposition from an acidic sulphate bath in the presence of chloride ions, PEG, SPS, and Benzyl-phenyl modified polyethyleneimine (BPPEI). The choice of the latter is based on our previous experience with benzyl-dimethyl-phenyl ammonium (BDMPA⁺) [Ph-N(CH₂)₂-CH₂-Ph]⁺ as an Au-plating additive [32–34]: we employed a functionalised polyethylene-imine type polymer containing the same quaternary ammonium functionality in the backbone as a model grain refiner for Cu plating [35–38]. The molecular scheme of this polymer is: $-\text{[CH}_2\text{-CH}_2\text{-N(Ph,CH}_2\text{-Ph)}^+\text{]}_x\text{-[CH}_2\text{-CH}_2\text{-N(CH}_2\text{-CH}_2\text{-NH}_2\text{)}_z\text{]}_y\text{-[CH}_2\text{-CH}_2\text{-NH]}_r\text{-}$.

Our electrochemical study is based on SERS, complemented by morphological SEM investigations of the effects of organic additives on the electroplated copper. To the best of our knowledge, many SERS studies related to single-additive containing bath have been published in [39–41]; however the behaviour of the entire blend, that is ultimately responsible for the quality of the coating, was not addressed by in situ spectroscopic study until now.

2 Experimental

The composition of the electrodeposition bath was: CuSO₄·5H₂O (Sigma Aldrich, Germany) 20 mM, H₂SO₄

L. D'Urzo (✉) · B. Bozzini
Dipartimento di Ingegneria dell'Innovazione, Università del Salento (Formerly Università di Lecce), Via Monteroni, Lecce 73100, Italy
e-mail: lucia.durzo@unile.it

0.5 M. To this solution we added: NaCl (Sigma Aldrich, Germany) 50 ppm, PEG MW 1500 (Fluka, Germany) 300 ppm, SPS (Raschig GmbH, Germany) 6 ppm and BPPEI specifically synthesized for this research, 10 mg L⁻¹. SERS measurements were performed with a LabRam confocal Raman system. Excitation at 633 nm was provided by a 12 mW He–Ne laser. A 50× long-working-distance objective was used. In situ spectroelectrochemistry was carried out in a cell with a vertical polycrystalline Cu disc working electrode of diameter 5 mm embedded in a Teflon cylindrical holder. The counter electrode was a Cu cylinder, coaxial with the working electrode holder. An Ag/AgCl (KCl 3 M) reference electrode was used, placed in a separate compartment; potentials are reported on the Ag/AgCl scale. The spectra acquisition time ranged between 30 and 60 s. The morphology of the samples was studied with a Cambridge Stereoscan 360 SEM. The electron source was LaB₆.

3 In situ surface enhanced Raman spectroscopy

SERS spectra were recorded at open circuit (OC) and 1, 2, 5, 6, 8 and 10 mA cm⁻². This range of current densities (c.d.s) corresponds to that typically adopted in industrial processes, implementing galvanostatic electrodeposition or sequences of c.d. ramps [42]. In Fig. 1 we show a typical spectrum obtained at open-circuit (0.056 mV). In this figure, the following features related to PEG were found:

- (i) Weak bands corresponding to the methylene group vibrations at: 1,220/1,270 cm⁻¹ (CH₂ twisting) and 1,420 cm⁻¹ (CH₂ scissoring) [43];
- (ii) Methylene asymmetric (2,925/2,970 cm⁻¹) stretching [43];

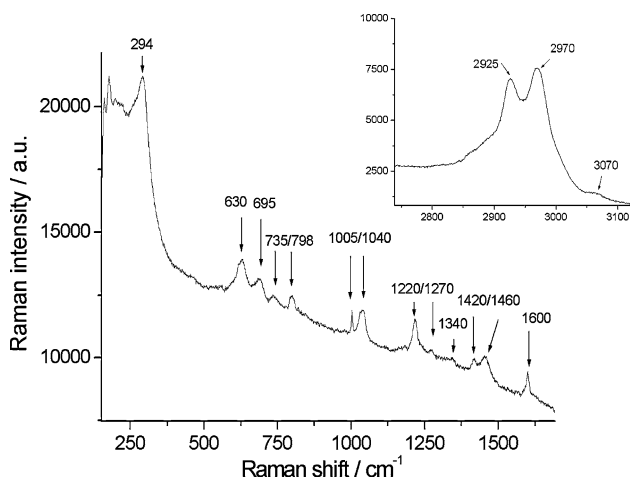


Fig. 1 In situ SERS spectra recorded at OC from a bath, containing 50 ppm Cl⁻, 300 ppm PEG, 6 ppm SPS, and 1 mg L⁻¹ BPPEI

- (iii) The weak broad band at 3,070 cm⁻¹ has been assigned to the stretching of the C–H bond in the RHC= group, owing the PEG fragmentation at the cathode during a multi step process that yields moieties containing vinyl ether group, as previously reported in [44–46].

As far as SPS is concerned, the following diagnostic features were identified [47–49]:

- (i) 630 cm⁻¹ assigned to C–S stretching;
- (ii) 695/735/798 cm⁻¹, assigned to SCH₂ rocking
- (iii) 1,040 cm⁻¹, assigned to the stretching of the sulfonic group.

Except for the strong band at 1,005 cm⁻¹, assigned to an aromatic ring stretching mode [32, 33, 37, 43], the identification of BPPEI features was in some cases complicated by the relatively poor signal intensity and some overlapping with CH₂ twisting and scissoring of PEG. Nevertheless, the stretching of the dimethyl aniline ring at 1,600 cm⁻¹ and the Ph–N stretching of quaternary ammonium at 1,340 cm⁻¹ can be unambiguously identified. The band at 1,460 cm⁻¹, assigned to semicircle stretching mixed with a C–H bending [43] mode, is better resolved at high current densities (see below and [38]).

The peak observed at 294 cm⁻¹ was assigned to Cu–O stretching [47–49], even though we are aware that Cu–O readily dissolves in acidic environment, nevertheless it is well known that surface-enhancement effects might be responsive to trace amounts of possibly transiently adsorbed species.

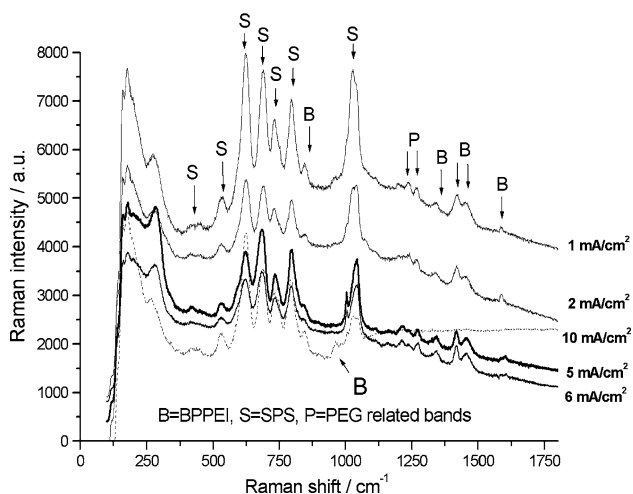
A list of the observed Raman bands, their indicative intensities and their assignments are provided in Table 1. When the bath was cathodically polarized at 1 mA/cm², we observed (Fig. 2):

- (i) A notable reduction of the SERS signal intensity, probably due to the formation of a fresh, but SERS-inactive copper layer;
- (ii) The intensity of the Cu–O stretching decreases, due to fresh copper deposition;
- (iii) Three new bands appeared at 425 cm⁻¹, 530 cm⁻¹ and 850 cm⁻¹, assigned respectively to C–S bending, SPS disulfide bridge stretching and to the SCH₂ deformations modes;
- (iv) The relative intensity of all other SPS bands increased;
- (v) The intensities of PEG-related CH₂ stretching (2,925/2,970 cm⁻¹) and vinyl-related CH stretching (3,070 cm⁻¹) tend to decrease or disappear [44–46].

Further spectral changes brought about by shifting the current from 1 to 10 mA cm⁻², can be summarised as follows (Figs. 2–4):

Table 1 Position, assignment and intensity of PEG, SPS and BPPEI bands

OC	1 mA cm ⁻²	2 mA cm ⁻²	5 mA cm ⁻²	6 mA cm ⁻²	10 mA cm ⁻²	Assignment
–	425 cm ⁻¹ , weak					C–S bending
–	530 cm ⁻¹ , weak					S–S stretching
630 cm ⁻¹ , medium-strong						C–S stretching and SO ₄ ⁻ bending band
695/735/798 cm ⁻¹ , medium-strong						SCH ₂ rocking
–	850 cm ⁻¹ , strong					Aromatic CH wag
–	–	–	–	–	960 cm ⁻¹ , weak	Out of plate C–H wagging [43]
1,005 cm ⁻¹ , strong						Ring stretching mode
1,040 cm ⁻¹						SO ₃ ⁻ symmetric stretching
1,220/1,270 cm ⁻¹ , weak to very weak						CH ₂ wagging and twisting
1,340 cm ⁻¹ , medium						Ph–N stretching for quaternary ammonium
1,420 cm ⁻¹ , weak to very weak						CH ₂ scissoring
1,460 cm ⁻¹ , medium						Semicircle stretching mixed with a C–H bending
1,600 cm ⁻¹ , medium						Ring stretching for dimethyl aniline
2,925/2,970 cm ⁻¹ , strong					–	CH ₂ asymmetric stretching
3,070 cm ⁻¹ , weak		–	–	–	–	Vinyl CH ₂ stretching

**Fig. 2** In situ SERS spectra recorded from a bath, containing 50 ppm Cl⁻, 300 ppm PEG, 6 ppm SPS, and 1 mg L⁻¹ BPPEI at the indicated current densities

(i) For Raman shifts lower than 1,000 cm⁻¹, strong SPS-related features show the adsorption of the salt in the entire cathodic window (Fig. 2). This result is consistent with our previous potentiostatic experiments, carried out in an acidic copper sulphate bath containing SPS in the presence and in the absence of Cl⁻ [48, 49]. As far as PEG is concerned, its typical carbonyl asymmetric stretching (at ~800 cm⁻¹) cannot be detected, due to its possible overlap with the stronger

SCH₂ deformation modes. At 10 mA cm⁻² a new small feature appears at 960 cm⁻¹, that can be assigned to the BPPEI out of plate CH wagging [43] (Fig. 2).

- (ii) For Raman shifts in the interval 1,000–2,800 cm⁻¹ the most prominent peak was found at ~1,040 cm⁻¹. All the features related to the methylene deformation of PEG exhibit a very low intensity that tends to decrease with increasing cathodic polarization. BPPEI bands can be observed, with weak or medium intensity (Fig. 2). The peak at 1,040 cm⁻¹ was found to be well approximated by a convolution of three Lorentzian peaks (Fig. 3), respectively assigned to: ring stretching mode of BPPEI aromatic groups (~1,005 cm⁻¹), vibration of PEG methylene groups (1,020 cm⁻¹ [44–46]) and stretching of SPS sulfonic termination (1,040 cm⁻¹). The relative intensities of these peaks change with the polarization. In particular, the ratio between the intensities of PEG- and SPS-related features tend to decrease as the c.d. increases, while the BPPEI band is better defined at higher c.d. values.
- (iii) For Raman shifts higher than 2,800 cm⁻¹, the band assigned to the vinyl CH₂ stretching disappears (Fig. 4). Overall, the intensity of methylene symmetric and asymmetric stretching bands decreases. No peaks related to SPS or BPPEI are present in this range.

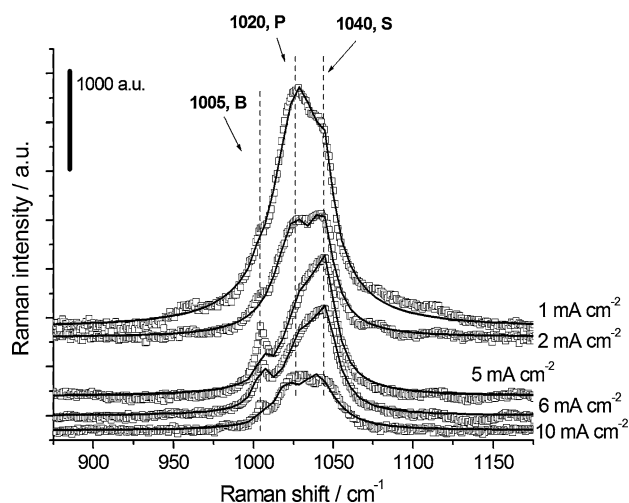


Fig. 3 In situ SERS spectra (range 900–1,250 cm^{-1}) recorded from a bath containing 50 ppm Cl^- , 300 ppm PEG, 6 ppm SPS, and 1 mg L^{-1} BPPEI at the indicated current densities. The spectra have been background-subtracted and shifted for clarity of presentation. The fits correspond to a three-Lorentzian model

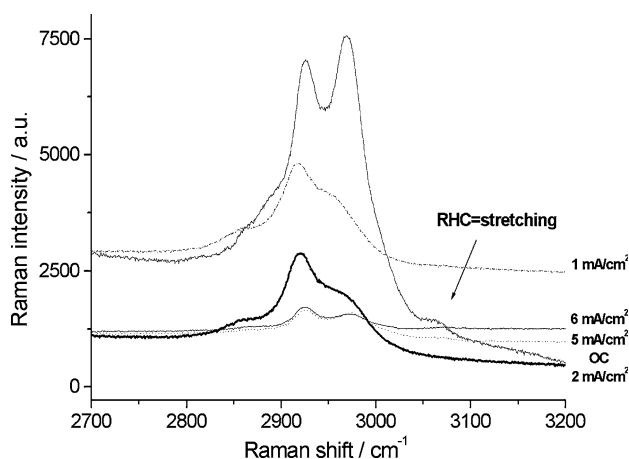


Fig. 4 In situ SERS spectra (range 2,700–3,200 cm^{-1}) recorded from a bath containing 50 ppm Cl^- , 300 ppm PEG, 6 ppm SPS, and 1 mg L^{-1} BPPEI at the indicated current densities

The analysis of our SERS spectra allows to get an insight into the complex behaviour of this organic mixture during the electroplating process. At open circuit, SPS, PEG and BPPEI bands clearly show the co-adsorption of the three additives on the electrode surface. Some moderate reactivity of PEG was also found coherently with the behaviour of baths containing PEG as the sole additive [44, 47]. The main reaction product has been identified in terms of polymer subunits containing the vinyl group R-CH=CH_2 as thoroughly discussed in [44–46]. When the cathodic polarisation is turned on, SPS features tend to dominate the spectra. We cannot identify any obvious changes in the spectral pattern that can demonstrate electroodic reaction of SPS. In particular, the stretching of the disulfide bridge was detectable at all c.d.s studied. These results are in good agreement with previous experiment carried out in the Copper electrodeposition bath containing SPS and Cl^- only [49]. As far as PEG is concerned, the peak assigned to vinyl as a polymer breakdown product tends to disappear already at 1 mA cm^{-2} . This fact can be explained with its incorporation into the growing cathode, in correspondence of non-SERS-active sites [36] or by desorption. Moreover, the SPS-scavenging action of PEG has been reported in [2], based on electrochemical measurements. Finally, the adsorption of BPPEI by its aromatic moieties is proven in the entire cathodic range covered in this experiment. No changes in the spectral pattern, suggesting polymer reactivity, could be detected.

4 Scanning electron microscopy

In Figs. 5 and 6 we show in-plane SEM micrographs of thick (thickness in excess of 30 μm) Cu layers deposited galvanostatically at 2 mA cm^{-2} from the following deposition baths:

- (i) $\text{CuSO}_4 \cdot 5\text{H}_2\text{O}$ 20 mM, H_2SO_4 0.5 M, NaCl 50 ppm, PEG MW 1500, 300 ppm, SPS 6 ppm and 3-

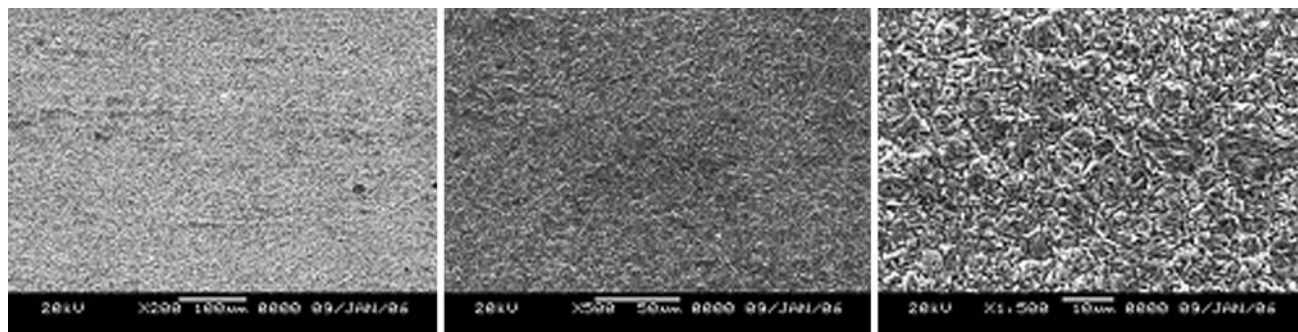


Fig. 5 SEM micrographs of Cu deposited from a solution containing $\text{CuSO}_4 \cdot 5\text{H}_2\text{O}$ 20 mM, H_2SO_4 0.5 M, NaCl 50 ppm, PEG MW 1500, 300 ppm, SPS 6 ppm and 3-Diethylamino-7-

(4-dimethylaminophenylazo)-5-phenylphenazinium chloride (Janus Green B, JGB) 1 mg L^{-1} , obtained at 2 mA cm^{-2} , magnification 200 \times , 500 \times , and 1,500 \times

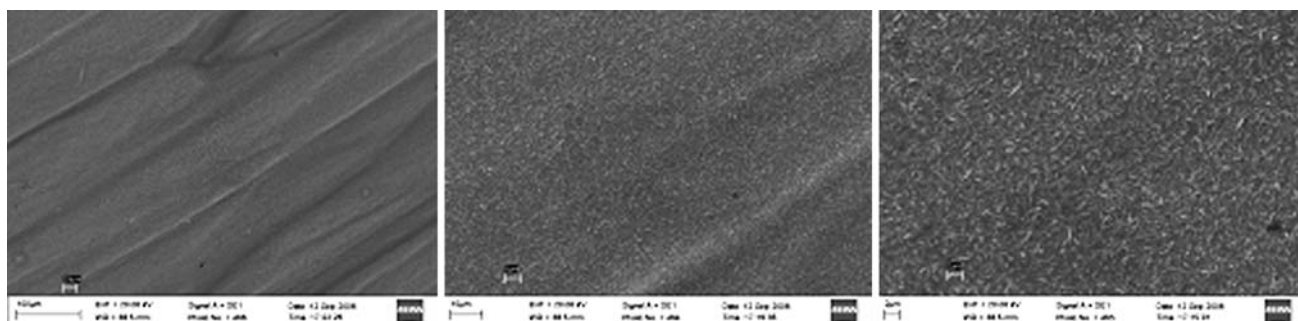


Fig. 6 SEM micrographs of Cu deposited from a solution containing $\text{CuSO}_4 \cdot 5\text{H}_2\text{O}$ 20 mM, H_2SO_4 0.5 M, NaCl 50 ppm, PEG MW 1500, 300 ppm, SPS 6 ppm and BPPEI 10 mg L^{-1} , obtained at 2 mA cm^{-2} , magnification: $500\times$, $1,500\times$, and $6,000\times$

- Diethylamino-7-(4-dimethylaminophenylazo)-5-phenylphenazinium chloride (Janus Green B, JGB) 1 mg L^{-1} ;
- (ii) $\text{CuSO}_4 \cdot 5\text{H}_2\text{O}$ 20 mM, H_2SO_4 0.5 M, NaCl 50 ppm, PEG MW 1500, 300 ppm, SPS 6 ppm and BPPEI 10 mg L^{-1} .

The former bath, containing a leveller widely studied in the literature [2, 38, 50], is commonly regarded as the benchmark for the evaluation of the grain refining power of innovative levellers. In the presence of JGB, a compact, grainy layer is obtained (Fig. 5). Primary crystallites, deriving from nucleation events, seem to split during growth into sub-grain domains. Overall, JGB at this c.d. exhibits a slight grain-refining activity (average grain dimension ca. $1\text{--}3.5 \mu\text{m}$). BPPEI, instead, shows a remarkable grain-refining effect. In the presence of the polymer, a continuous layer is obtained. Pictures taken at high magnification ($3,000\times$ and $6,000\times$) reveal the formation of elongated crystallites, of submicron dimensions (Fig. 6).

SERS data measured during Cu electroplating from JGB-containing baths have been reported in [45, 48]. It can be noticed that quality of the spectra measured in the presence of BPPEI is higher with respect to that of corresponding to use of JGB. This result does not relate straightforwardly to the mesoscopic morphology assessed by SEM. The grainier deposits grown from the JGB bath in fact do not seem to give rise to a higher surface enhancement than the tinier features developing in the BPPEI bath. This hints at the fact that the hot-spots allowing surface-enhancement in the present case might exhibit nanometric dimensions.

5 Conclusions

The synergistic behaviour of PEG, SPS and BPPEI during galvanostatic copper electrodeposition can be summarized as follows:

- (i) at open-circuit, accelerator, suppressor and leveller co-adsorb on the copper cathode.
- (ii) when the cathodic polarization is applied, the relative surface coverage between SPS and PEG increases with the polarization; BPPEI-related bands are present in the entire process window and look better defined at higher c.d.;
- (iii) the joint action of the organic additives yields a continuous deposit. Compared to the benchmark leveller JGB, BPPEI allowed the formation of crystallites of submicron dimensions.

To the best of the authors' knowledge, the simultaneous action of all the types of additives used for the electrodeposition of Cu interconnects during a galvanostatic process mimicking a state-of-art manufacturing process has been clarified at a molecular level for the first time in this research.

Acknowledgements Highly qualified and continuous technical assistance with electrochemical experiments and SEM are kindly acknowledged to Francesco Bogani and Donato Cannoletta (Dipartimento di Ingegneria dell'Innovazione, Università di Lecce, Italy), respectively

References

1. J. Reid, C. Gack, J. Hearne, *Electrochem. Solid-State Lett.* **6**(2), C26–C29 (2003). doi:10.1149/1.1535754
2. P. Taephaisitphonse, A. West, *J. Electrochem. Soc.* **148**(7), C492–C497 (2001). doi:10.1149/1.1376636
3. J. Kelly, C. Tian, A. West, *J. Electrochem. Soc.* **146**(7), 2540–2545 (1999). doi:10.1149/1.1391968
4. J. Kelly, A. West, *J. Electrochem. Soc.* **2**(11), 561–563 (1999)
5. T.P. Moffat, J.E. Bonevich, W.H. Huber, A. Stanishevsky, D.R. Kelly, G.R. Stafford, D. Jossel, *J. Electrochem. Soc.* **147**(12), 4524–4535 (2000). doi:10.1149/1.1394096
6. M. Yokoi, S. Konishi, T. Hayashi, *Denki Kagaku* (English edition). **52**, 218 (1984)
7. K.R. Hebert, S. Adhikari, J.E. Houser, *J. Electrochem. Soc.* **152**(5), C324–C329 (2005)
8. J.P. Healy, D. Pletcher, M. Goodenough, *J. Electroanal. Chem.* **338**, 155–165 (1992). doi:10.1016/0022-0728(92)80420-9

9. D. Stoychev, C. Tsvetanov, *J Appl Electrochem.* **26**, 741–749 (1996). doi:[10.1007/BF00241515](https://doi.org/10.1007/BF00241515)
10. J.J. Kelly, A.C. West, *J. Electrochem. Soc.* **145**, 3472 (1998). doi:[10.1149/1.1838829](https://doi.org/10.1149/1.1838829)
11. J.J. Kelly, A.C. West, *J. Electrochem. Soc.* **145**, 3477 (1998). doi:[10.1149/1.1838830](https://doi.org/10.1149/1.1838830)
12. Y. Cao, P. Taephaisitphongse, R. Chalupa, A.C. West, *J. Electrochem. Soc.* **148**, 466 (2001). doi:[10.1149/1.1377898](https://doi.org/10.1149/1.1377898)
13. J.J. Kelly, A.C. West, *Electrochem. Solid-State Lett.* **2**, 561 (1999). doi:[10.1149/1.1390904](https://doi.org/10.1149/1.1390904)
14. K. Kondo, K. Hayashi, Z. Tanaka, N. Yamakawa, in *Electrochemical Processing in ULSI Fabrication III*, ed. by P.C. Andricacos, J.L. Stickney, P.C. Searson, C. Reidsema-Simson, G.M. Oleszek, ECS Proc. vol. 2000-8, p. 76
15. J. Horkans, J.O. Dukovic, in *Electrochemical Processing in ULSI Fabrication III*, ed. by P.C. Andricacos, J.L. Stickney, P.C. Searson, C. Reidsema-Simson, G.M. Oleszek, ECS Proc. vol. 2000-8, p. 103
16. J. Reid, S. Mayer, E. Broadbent, E. Klawuhn, K. Ashtiani, *Solid State Technol.* **43**, 86 (2000)
17. S. Miura, K. Oyamada, S. Watanabe, M. Sugimoto, H. Kouzai, H. Honma, in *Copper Interconnects, New Contact Metallurgies, Structures, and Low-k Interlevel Dielectrics*, ed. by G.S. Mathad, ECS Proc. vol. 2002-22, p. 22
18. T.P. Moffat, D. Wheeler, C. Witt, D. Josell, *Electrochem. Solid-State Lett.* **5**, C110 (2002). doi:[10.1149/1.1521290](https://doi.org/10.1149/1.1521290)
19. A. Radisic, A.C. West, P.C. Searson, *J. Electrochem. Soc.* **149**, C94 (2002). doi:[10.1149/1.1430719](https://doi.org/10.1149/1.1430719)
20. M. Tan, J. Hutchins, J.N. Harb, in *Copper Interconnects, New Contact Metallurgies, Structures, and Low-k Interlevel Dielectrics*, ed. by G.S. Mathad, ECS Proc. vol. 2002-22, p. 15
21. W.-P. Dow, H.-S. Huang, Z. Lin, *Electrochem. Solid-State Lett.* **6**, C134 (2003). doi:[10.1149/1.1595311](https://doi.org/10.1149/1.1595311)
22. A. Frank, A.J. Bard, *J. Electrochem. Soc.* **150**, C244 (2003). doi:[10.1149/1.1557081](https://doi.org/10.1149/1.1557081)
23. M. Kang, A.A. Gewirth, *J. Electrochem. Soc.* **150**, C426 (2003). doi:[10.1149/1.1572152](https://doi.org/10.1149/1.1572152)
24. J.J. Kim, S.-K. Kim, Y.S. Kim, *J. Electroanal. Chem.* **542**, 61 (2003). doi:[10.1016/S0022-0728\(02\)01450-X](https://doi.org/10.1016/S0022-0728(02)01450-X)
25. K. Kondo, N. Yamakawa, Z. Tanaka, K. Hayashi, *J. Electroanal. Chem.* **559**, 137 (2003). doi:[10.1016/S0022-0728\(03\)00110-4](https://doi.org/10.1016/S0022-0728(03)00110-4)
26. S. Miura, H. Honma, *Surf. Coat. Technol.* **169–170**, 91 (2003). doi:[10.1016/S0257-8972\(03\)00165-8](https://doi.org/10.1016/S0257-8972(03)00165-8)
27. T.P. Moffat, B. Baker, D. Wheeler, D. Josell, *Electrochem. Solid-State Lett.* **6**, C59 (2003). doi:[10.1149/1.1553936](https://doi.org/10.1149/1.1553936)
28. M. Tan, J.N. Harb, *J. Electrochem. Soc.* **150**, C420 (2003). doi:[10.1149/1.1570412](https://doi.org/10.1149/1.1570412)
29. K. Kondo, T. Matsumoto, K. Watanabe, *J. Electrochem. Soc.* **151**, C250 (2004). doi:[10.1149/1.1649235](https://doi.org/10.1149/1.1649235)
30. T.P. Moffat, D. Wheeler, D. Josell, *J. Electrochem. Soc.* **151**, C262 (2004). doi:[10.1149/1.1651530](https://doi.org/10.1149/1.1651530)
31. J. Reid, J. Zhou, 209th ECS Meeting, May 7–12, 2006, Denver, Colorado (2006)
32. A. Fanigliulo, B. Bozzini, *J. Electroanal. Chem.* **530**, 53 (2002). doi:[10.1016/S0022-0728\(02\)00995-6](https://doi.org/10.1016/S0022-0728(02)00995-6)
33. A. Fanigliulo, B. Bozzini, *Electrochim. Acta* **47**, 4511 (2002). doi:[10.1016/S0013-4686\(02\)00538-8](https://doi.org/10.1016/S0013-4686(02)00538-8)
34. B. Bozzini, A. Fanigliulo, *Trans. IMF.* **80**, 25 (2002)
35. B. Bozzini, L. D'Urzo, G. Giovannelli, C. Mele, V. Romanello, 207th ECS Meeting, May 14–20, 2005, Quebec City, Canada (2005)
36. B. Bozzini, B. Busson, G.P. De Gaudenzi, L. D'Urzo, G. Giovannelli, C. Mele, C. Six, F. Vidal, A. Tadjeddine, 207th ECS Meeting, May 14–20, 2005, Quebec City, Canada (2005)
37. B. Bozzini, L. D'Urzo, C. Mele, *Electrochim. Acta* **52**, 4767 (2007). doi:[10.1016/j.electacta.2007.01.015](https://doi.org/10.1016/j.electacta.2007.01.015)
38. B. Bozzini, C. Mele, L. D'Urzo, V. Romanello, G. Giovannelli, *Trans. IMF.* **84**, 177–187 (2006)
39. G.A. Hope, R. Woods, *J. Electrochem. Soc.* **151**(9), C550–C553 (2004)
40. Z.D. Schultz, Z.V. Feng, M.E. Biggin, A.A. Gewirth, *Electrochem. Soc.* **153**(2), C97–C107 (2006)
41. J.P. Healy, D. Pletcher, and M. Goodenough, (a) *J. Electroanal. Chem.* **338**, 167 (1992); (b) *J. Electroanal. Chem.* **338**, 179, (1992). doi:[10.1016/0022-0728\(92\)80422-Z](https://doi.org/10.1016/0022-0728(92)80422-Z)
42. G. Banerjee, J. So, B. Mikkola, *Solid State Technol.* November (2001)
43. N.B. Colthup, L.H. Daly, S.E. Wiberley, *Introduction to Infrared and Raman Spectroscopy* (Academic Press, Boston, 1990)
44. B. Bozzini, L. D'Urzo, G. Giovannelli, C. Mele, *Trans. IMF.* **82**, 118 (2004)
45. B. Bozzini, C. Mele, L. D'Urzo, *J. Appl. Electrochem.* **36**, 789–800 (2006). doi:[10.1007/s10800-006-9139-6](https://doi.org/10.1007/s10800-006-9139-6)
46. B. Bozzini, L. D'Urzo, C. Mele, V. Romanello, *J Mater. Sci. Mater. Electron.* **17**, 915–923 (2006). doi:[10.1007/s10854-006-0044-x](https://doi.org/10.1007/s10854-006-0044-x)
47. K. Nakamoto, *Infrared and Raman Spectra of Inorganic and Coordination Compounds.* (Wiley, NY, 1997) pp. 187–90, Part B
48. B. Bozzini, L. D'Urzo, C. Mele, V. Romanello, *Trans. IMF.* **84**, 83–93 (2006)
49. B. Bozzini, L. D'Urzo, C. Mele, V. Romanello, *J. Electrochem. Soc.* **153**, C254 (2006). doi:[10.1149/1.2172555](https://doi.org/10.1149/1.2172555)
50. B. Bozzini, C. Mele, L. D'Urzo, V. Romanello, *J. Appl. Electrochem.* **36**, 973–981 (2006). doi:[10.1007/s10800-006-9124-0](https://doi.org/10.1007/s10800-006-9124-0)